

Formation of current sheets and sigmoidal structure by the kink instability of a magnetic loop

B. Kliem¹, V. S. Titov², and T. Török^{1,3}

¹ Astrophysikalisches Institut Potsdam, 14482 Potsdam, Germany

² Theoretische Physik IV, Ruhr-Universität Bochum, 44780 Bochum, Germany

³ School of Mathematics and Statistics, University of St Andrews, St Andrews, Fife KY16 9SS, UK

Received 4 April 2003 / Accepted 3 November 2003

Abstract. We study dynamical consequences of the kink instability of a twisted coronal flux rope, using the force-free coronal loop model by Titov & Démoulin (1999) as the initial condition in ideal-MHD simulations. When a critical value of the twist is exceeded, the long-wavelength ($m=1$) kink mode develops. Analogous to the well-known cylindrical approximation, a helical current sheet is then formed at the interface with the surrounding medium. In contrast to the cylindrical case, upward-kinking loops form a second, vertical current sheet below the loop apex at the position of the hyperbolic flux tube (generalized X line) in the model. The current density is steepened in both sheets and eventually exceeds the current density in the loop (although the kink perturbation starts to saturate in our simulations without leading to a global eruption). The projection of the field lines that pass through the vertical current sheet shows an S shape whose sense agrees with the typical sense of transient sigmoidal (forward or reverse S-shaped) structures that brighten in soft X rays prior to coronal eruptions. The upward-kinked loop has the opposite S shape, leading to the conclusion that such sigmoids do not generally show the erupting loops themselves but indicate the formation of the vertical current sheet below them that is the central element of the standard flare model.

Key words. Instabilities – Magnetic fields – MHD – Sun: corona – Sun: coronal mass ejections (CMEs) – Sun: flares

1. Introduction

Rising filaments, flares, and coronal mass ejections on the Sun often show the phenomenology of a loop-shaped magnetic flux system with fixed footpoints at the coronal base and signatures of magnetic twist. A single twisted magnetic flux rope appears to contain essential elements of the magnetic topology of the unstable, often erupting flux. Since the ratio of kinetic to magnetic pressure, the plasma beta, is very small in the inner corona, $\beta \sim 10^{-3} \dots 10^{-2}$, the flux system must be nearly force free in the quasi static pre-eruption state, i.e.,

$$\nabla \times \mathbf{B} = \alpha(x) \mathbf{B}. \quad (1)$$

Such major energy release events, which we will refer to collectively as flares in the following, often show a distinctive soft X-ray (SXR) brightening of sigmoidal (S or reverse-S) shape shortly prior or during their early, impulsive stages of development (e.g., Rust & Kumar, 1996; Manoharan et al., 1996; Pevtsov et al., 1996; Aurass et al., 1999; Moore et al., 2001; Gibson et al., 2002). The sigmoidal shape is generally regarded as a signature of coronal currents in a twisted field and shows a hemispheric preference: forward (reverse) S shapes dominate in the southern (northern) hemisphere (Rust & Kumar, 1996). Typically the central part of such transient sigmoids is ap-

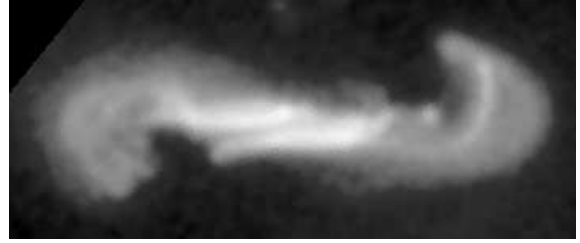


Fig. 1. Transient sigmoid observed in an eruptive flare on 1994 Oct 25 (from Manoharan et al., 1996) in AR 7792, which had primarily left-handed twist (Aurass et al., 1999; van Driel-Gesztelyi et al., 2000).

proximately aligned with the neutral line of the normal photospheric field component, often also with a filament. They are bright and more sharply defined in the middle, while their ends fan out more diffusively at opposite sides of the neutral line. Sometimes their middle section is slightly split, giving the structure the appearance of two point-symmetric letters J. Each J may consist of several fibres (Fig. 1).

The solar soft X-ray corona often also contains long-lived sigmoidal structures that appear to form a separate class. These typically exist for more than a day, do not show the concentration in the middle, may be composed of many fibres that show

the S shape collectively rather than individually, and may form not only within but also between active regions.

The sense of the sigmoidal shape and the handedness of the magnetic twist are correlated: Pevtsov et al. (1997) found that more than 90% of all sigmoids in those active regions that have a uniform sign of α in the photospheric magnetogram show forward (reverse) S shape for $\alpha > (<) 0$, i.e., for right (left) handed twist. We will refer to this result as σ - α correlation, where $\sigma > (<) 0$ stands for forward (reverse) S shape. The correlation is consistent with the hemispheric preference, since α is predominantly $> (<) 0$ in the southern (northern) hemisphere (Seehafer, 1990; Pevtsov et al., 1995).

The transient sigmoids that brighten in flares (both confined and eruptive) have so far mostly been interpreted as an illumination of the unstable flux system itself. Rust & Kumar (1996) proposed that they show a sufficiently twisted, kink-unstable flux rope. Pevtsov et al. (1996), Moore et al. (2001), and others suggested further that the unstable flux rope acquired its super-critical twist through the reconnection of two nearly aligned, subcritical flux ropes near their end points, which conforms to the strong brightening in the middle of the sigmoids and may symbolically be written as $J + J \rightarrow S$. Transient sigmoids were thus regarded by Moore et al. (2001) as supporting their “tether cutting” model of flares (although they noted that another, much fainter structure was moving in sequences of SXR images in some of their events).

The presence of a SXR sigmoid correlates with the likelihood of a flaring active region to cause an eruption (Canfield et al., 1999). A “standard” model for the main phase of eruptive flares is now widely accepted (e.g., Shibata, 1999). It includes the formation of a large-scale vertical current sheet below the erupting flux, in which magnetic reconnection leads to the long-lasting energy release. This model is assumed to hold independently of the question whether the event is initiated by an instability of a single flux rope, by reconnection between flux ropes (tether cutting), or by other mechanisms, e.g., “magnetic breakout” (Antiochos et al., 1999).

The canonical instability of a twisted flux rope is the kink instability. In applications to the solar corona, the simplifying assumption of straight, cylindrically symmetric flux ropes has always been used so far (e.g., Hood, 1992). This is based on the typically large aspect ratio of solar magnetic loops. The instability occurs if the twist, $\Phi = lB_\phi(r)/(rB_z(r))$, exceeds a critical value, Φ_c . Here l is the length of the flux rope, r is the (minor) radius, and B_z and B_ϕ are the axial and azimuthal field components, respectively. The critical value depends on the details of the considered equilibrium.

In this paper we address the relationship between the kink instability of an arched twisted flux rope and the formation of current sheets and sigmoidal structures, starting from the analytical magnetic loop equilibrium by Titov & Démoulin (1999), cited as T&D in the following (see their Fig. 2 for a schematic). This approximate, cylindrically symmetric, force-free equilibrium consists of a toroidal ring current of major radius R and minor radius a , whose outward-directed Lorentz self-force is balanced with the help of a field by two fictitious magnetic charges of opposite sign which are placed at the symmetry axis of the torus at distances $\pm L$ to the torus plane. That

axis lies below the photospheric plane $\{z=0\}$ at a depth d . The resulting field outside the torus is current-free and contains a concentric magnetic X line between the torus and its centre. A toroidal field component created by a fictitious line current running along the axis of symmetry is added. This results in a force-free field inside the torus with the twist taking a finite value everywhere in the configuration, whose part in the volume $\{z>0\}$ is a model of a coronal loop (or flux rope).

The presence of a toroidal field component turns the neighbourhood of the X line into a hyperbolic flux tube (HFT) which consists of two intersecting quasi-separatrix layers with extremely diverging field lines (for a strict definition of HFTs, see Titov et al., 2002). The existence of the HFT is generic to such force-free loop configurations with a nonvanishing net current (Titov et al., 1999), which is important for understanding the origin of sigmoidal structures in twisted configurations.

We present two characteristic cases of the kink instability, which show the different possibilities of current sheet and sigmoid formation in the T&D equilibrium, leaving a systematic study of the instability for a separate paper (Török et al., 2003).

T&D pointed out that the torus is also unstable with respect to global expansion (growing perturbations $\delta R > 0$). This has recently been confirmed by Roussev et al. (2003). We expect that the global expansion instability leads to current sheets and sigmoidal structures in a manner largely analogous to the upward kink instability.

We integrate the compressible ideal MHD equations using the simplifying assumption $\beta = 0$ which has no influence on the qualitative evolution of the kink instability in its linear phase, during which the current sheets and sigmoids are formed:

$$\partial_t \rho = -\nabla \cdot (\rho \mathbf{u}), \quad (2)$$

$$\rho \partial_t \mathbf{u} = -\rho (\mathbf{u} \cdot \nabla) \mathbf{u} + \mathbf{j} \times \mathbf{B}, \quad (3)$$

$$\partial_t \mathbf{B} = \nabla \times (\mathbf{u} \times \mathbf{B}), \quad (4)$$

$$\mathbf{j} = \mu_0^{-1} \nabla \times \mathbf{B}. \quad (5)$$

The equilibrium by T&D is used as the initial condition for the field, with the loop chosen to lie in the plane $\{x=0\}$. The initial density distribution is specified such that the Alfvén velocity is uniform, $\rho_0 = B_0^2/\mu_0$. Lengths, velocities, and times are normalized, respectively, by L , the initial Alfvén velocity, $v_{a0} = B_0/(\mu_0 \rho_0)^{1/2}$, and the Alfvén time, $\tau_a = L/v_{a0}$.

A modified Lax-Wendroff scheme is employed on a nonuniform Cartesian grid in a “half cube” $[-L_x, L_x] \times [0, L_y] \times [0, L_z]$ with closed boundaries except the front boundary, $\{y=0\}$, where line symmetry with respect to the z axis is implemented. The latter implies $u_{x,y}(0, 0, z) = 0$ so that only vertical displacements of the loop apex are permitted. Viscosity is included in Eq. (3) to improve numerical stability. The numerical details are the same as in Török et al. (2003).

2. Kink instability

The parameters of the basic loop equilibrium are chosen similarly to T&D: $d = L = 1$ (50 Mm) and $R = 2.2$. The twist is specified via the number of turns that the field lines at the surface of the torus make about its axis (counted for the whole

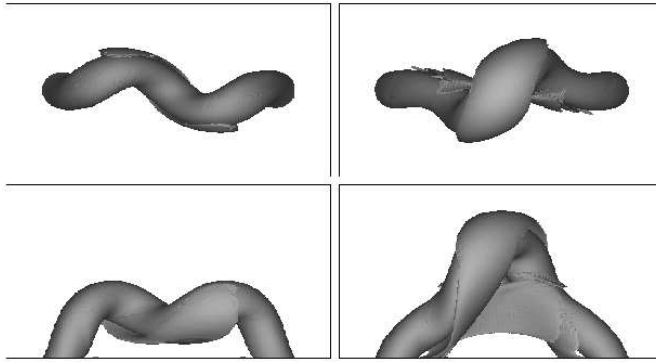


Fig. 2. Top and side view of current density isosurfaces for $\Phi = 4.9\pi$. *Left:* $|j| = 0.15 j_{\max}$ at $t = 35$; unperturbed case. *Right:* $|j| = 0.25 j_{\max}$ at $t = 28$; run with an upward initial velocity perturbation at the loop apex. $|x| \leq 1.5$, $|y| \leq 3$, $0 \leq z \leq 3$.

torus), taken here to be $N_t = 15$. This also fixes the minor radius of the loop, $a = 0.32$. The resulting twist of the coronal part of the loop, averaged over its cross section, $\Phi = 4.9\pi$, is about $1.4\Phi_c$ of this configuration (Török et al., 2003). Here the long-wavelength ($m = 1$) kink mode develops spontaneously with downward displacement of the loop apex; it is initiated by the weak, downward-directed forces that result from the initial discretization errors of the current density on the grid. The displacement and velocity of the apex rise exponentially until the apex height is reduced to $\approx 2/3$ of its initial value by $t \approx 25$, after which the instability starts to saturate. The configuration that results for left-handed twist ($\alpha < 0$) is shown in Fig. 2 (left) by current density isosurfaces. The kink perturbation forms a helical current sheet that is wrapped around the displaced parts of the loop at the interface with the surrounding plasma in a manner similar to the cylindrical case. The current density in this sheet rises exponentially as well, eventually exceeding the current density in the loop. The projection of both the loop and the current sheet onto the bottom plane possess a reverse S shape, as is characteristic of sigmoids in left-handed twisted fields. If the handedness of the twist is reversed, then the $m = 1$ kink mode develops with identical time profile but reversed handedness of the loop perturbation, i.e., forward S shape of its photospheric projection.

In order to study the kink mode with upward apex displacement, a small upward initial velocity perturbation is applied at the apex. It is ramped up over $5\tau_a$ to $u_z = 0.01$, then switched off. In this run the $m = 1$ kink mode develops with a similar growth rate as before, but again starts to saturate after $t \approx 25$, at an apex velocity of $u_z \approx 0.1$. The resulting configuration in the case of left-handed twist is also shown in Fig. 2 (right). In addition to the helical current sheet that is again formed as the kink perturbation piles up the surrounding flux, a second current sheet, which has no analogue in the cylindrical case (but corresponds to the main element of the standard flare model), now occurs below the rising section of the loop. It is formed by a pinching of the HFT in the lateral stagnation flow set up below the rising loop apex. For a detailed analysis of the pinching mechanism, which is a three-dimensional generalization of the well-known pinching of X points in the 2D case, we refer

to Titov et al. (2003) and Galsgaard et al. (2003). The current density rises exponentially in both sheets, exceeding that in the kinked loop in the nonlinear stage of the instability. The rising unstable loop and the helical current sheet now both possess a forward S-shaped photospheric projection – opposite to the characteristic sigmoid shape in left-handed fields. Reversing the twist of the initial configuration leads to the upward $m = 1$ kink mode with identical time profile but reversed handedness of the kink perturbation. It should be noted that the applied velocity perturbation is exactly vertical and so does not introduce a preference for the handedness of the kink perturbation. The two configurations of opposite sigmoidal shape shown in Fig. 2 possess the same photospheric α .

3. Formation of sigmoids

In all four cases discussed in the previous section, the handedness of the kink perturbation of the loop axis (sign of “external writhe”) equals the handedness of the field line twist (sign of “internal writhe”). This is a general property of the kink instability (known as resonance at the point of marginal stability; see, e.g. Linton et al., 1999). Its immediate consequence is that *transient sigmoids cannot be identified with rising kink-unstable loops*. Since there are strong observational indications for the existence of substantial magnetic twist in eruptive flux systems, transient sigmoids must in general be associated with another structure in the unstable twisted flux.

We follow the suggestion by T&D that bright SXR structures outline magnetic structures with enhanced current density, and hence enhanced dissipation, and calculate field lines that pass through the vertical current sheet below the upward-rising kinked loop (Figs. 3 and 4). These field lines form a sigmoidal surface that not only follows the σ - α correlation but also corresponds nicely to further properties of transient sigmoids like the near-alignment with the photospheric neutral line, the concentration in the middle and the diffuse spreading at the ends. The occasionally observed splitting into two J-shaped parts, which may themselves consist of multiple J-shaped fibres, can readily be explained by assuming the existence of multiple current density peaks within the current sheet. This can naturally be expected in a fibrous corona (we have indicated this effect in Figs. 3 and 4 by selecting field lines that pass closely to the z axis; in our simulation of a smooth initial configuration, the current density peaks exactly at the z axis). Flux pileup in the stagnation flow at both sides of the current sheet may also lead to the effect. Finally, cases of sigmoid lengthening, as described by Manoharan et al. (1996), are consistent with the new interpretation only.

Magnetic reconnection is expected to occur in the vertical current sheet, amplifying the brightening of the sigmoidal field lines at SXR and permitting transitions between continuous (S) and broken (double J) sigmoidal patterns (in both directions).

With this interpretation, transient sigmoids cannot be considered as direct support of the tether cutting model (Moore et al., 2001) but, of course, they do not contradict the model in any manner. Our interpretation is not undermined by the fact that the kink-unstable loop does not succeed to evolve

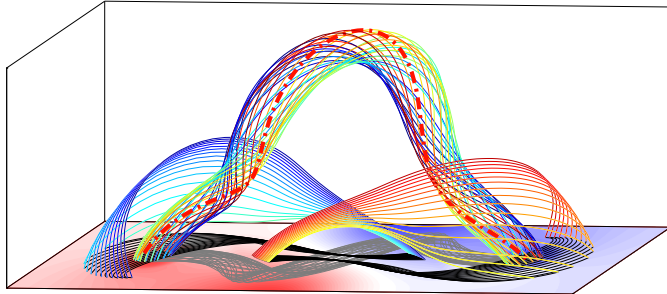


Fig. 3. Field lines of the configuration shown in the right panels of Fig. 2. $|x| \leq 0.8$, $|y| \leq 3$, $0 \leq z \leq 2.2$. Loop field lines lie in the surface $r = a/2$ (to separate the loop clearly from the sigmoids); one of them is emphasized to indicate the left handedness of the twist. The remaining field lines pass through two symmetrical vertical stripes close to the z axis that bracket the pinched HFT. The normal component of the magnetic field in the bottom plane is shown color-coded (blue – positive, red – negative). Projections of the field lines are overlaid.

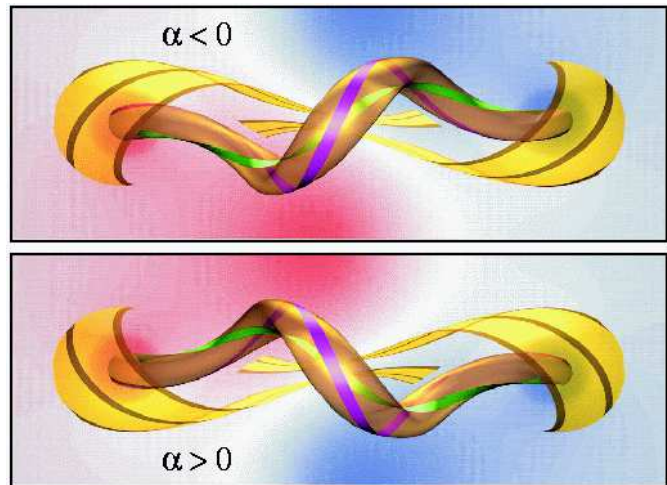


Fig. 4. Top view on selected field lines and on the surfaces that they form. $|x| \leq 1$, $|y| \leq 3$. The field lines for $\alpha < 0$ are identical to those plotted in Fig. 3. The bottom panel shows similarly selected field lines of the system with reversed α at the same time.

into a true eruption in our simulations (Török et al., 2003), because transient sigmoids occur at the onset of eruptive events.

The downward-kinked loop may be associated with long-lived sigmoids. As the instability saturates, this kink perturbation may lead to a stable structure which follows the σ - α correlation and is nearly aligned in the middle with the photospheric neutral line. The dip in the loop or in the flux below it supports the formation of a filament, which is often observed in close spatial association with sigmoids (Pevtsov, 2002). Further studies are required to check this conjecture. See Török & Kliem (2003) for an alternative interpretation of long-lived sigmoids as loops of enhanced current density but subcritical twist.

4. Conclusions

The magnetic loop equilibrium by T&D is unstable against the long-wavelength ($m = 1$) ideal kink mode if the magnetic twist exceeds a critical value. The handedness of the kink perturbation equals the handedness of the field line twist. Consequently, the photospheric projection of rising kink-unstable loops develops a forward (reverse) S shape for left (right) handed twist. This is opposite to the strong observed (σ - α) correlation of sigmoid shape with magnetic handedness. Hence, transient SXR sigmoids, which brighten in major energy release events, preferably in eruptive events, cannot in general show the presumed kink-unstable flux itself. We suggest that transient sigmoids outline field lines which pass through the current density enhancement in a vertical current sheet formed below the rising loop. This interpretation leads to agreement with the σ - α correlation (and hemispheric preference) as well as with their alignment with the photospheric neutral line and with their further specific geometric properties. Transient sigmoids thus indicate the formation of the vertical current sheet that is the central element of the standard model for eruptive flares. The question under which conditions a rising kink-unstable loop develops into an eruption requires further study.

Downward-kinking loops take a sigmoidal shape that follows the observed correlation with handedness. They may be related to long-lived sigmoids and to filament formation.

Acknowledgements. We thank R. J. Leamon for pointing out the relationship of our calculations to the model by Rust & Kumar (1996). This investigation was supported by BMBF/DLR grants No. 50 OC 9901 2 and 01 OC 9706 4, by the Volkswagen Foundation, and by EU grant No. HPRN-CT-2000-00153. The John von Neumann-Institut für Computing, Jülich granted Cray computer time.

References

- Antiochos, S. K., DeVore, C. R., & Klimchuk, J. A. 1999, *ApJ*, 510, 485
- Aurass, H., Vršnak, B., Hofmann, A., & Rudžjak, V. 1999, *Sol. Phys.*, 190, 267
- Canfield, R. C., Hudson, H. S., & McKenzie, D. E. 1999, *Geophys. Res. Lett.*, 26, 627
- Galsgaard, K., Titov, V. S., & Neukirch, T. 2003, *ApJ*, 595, 506
- Gibson, S. E. et al. 2002, *ApJ*, 574, 1021
- Hood, A. W. 1992, *Plasma Phys. & Contr. Fusion*, 34, 411
- Linton, M. G., Fisher, G. H., Dahlburg, R. B., & Fan, Y. 1999, *ApJ*, 522, 1190
- Manoharan, P. K., van Driel-Gesztelyi, L., Pick, M., & Démoulin, P. 1996, *ApJ*, 468, L73
- Moore, R. L., Sterling, A. C., Hudson, H. S. & Lemen, J. R. 2001, *ApJ*, 552, 833
- Pevtsov, A. A. 2002, *Sol. Phys.*, 207, 111
- Pevtsov, A. A., Canfield, R. C., & Metcalf, T. R. 1995, *ApJ*, 440, L109
- Pevtsov, A. A., Canfield, R. C., & Zirin, H. 1996, *ApJ*, 473, 533
- Pevtsov, A. A., Canfield, R. C., & McClymont, A. N. 1997, *ApJ*, 481, 973
- Roussev, I. I., et al. 2003, *ApJ*, 588 L45
- Rust, D. M., & Kumar, A. 1996, *ApJ*, 464, L199

Seehafer, N. 1990, Sol. Phys., 125, 219

Shibata, K. 1999, Ap&SS, 264, 129

Titov, V. S., & Démoulin, P. 1999, A&A, 351, 707 (T&D)

Titov, V. S., Démoulin, P., & Hornig, G. 1999, in Magnetic Fields & Solar Processes, ed. A. Wilson (ESA SP-448) 715

Titov, V.S., Galsgaard, K., & Neukirch, T. 2003, ApJ, 582, 1172

Titov, V. S., Hornig, G., & Démoulin, P. 2002, J. Geophys. Res., 107, doi:10.1029/2001JA000278

Török, T., & Kliem, B. 2003, A&A, 406, 1043

Török, T., Kliem, B., & Titov, V. S. 2003, A&A, in press

van Driel-Gesztelyi, L., Manoharan, P. K., Démoulin, P., et al. 2000, J. Atmospheric & Solar Terr. Phys., 62, 1437